




Article

# Hydrochloric Acidic Processing of Titanite Ore to Produce a Synthetic Analogue of Korobitsynite

Lidia G. Gerasimova <sup>1,2</sup>, Anatoly I. Nikolaev <sup>1,2</sup>, Ekaterina S. Shchukina <sup>1,2</sup>,  
Marina V. Maslova <sup>1,2</sup>, Galina O. Kalashnikova <sup>1</sup>, Gleb O. Samburov <sup>3</sup> and  
Gregory Yu. Ivanyuk <sup>1,\*</sup>

<sup>1</sup> Nanomaterials Research Centre of Kola Science Centre, Russian Academy of Sciences, 14 Fersman Street, 184209 Apatity, Russia; gerasimova@chemy.kolasc.net.ru (L.G.G.); nikol\_ai@chemy.kolasc.net.ru (A.I.N.); shuki\_es@chemy.kolasc.net.ru (E.S.S.); maslova@chemy.kolasc.net.ru (M.V.M.); galka27\_89@mail.ru (G.O.K.)

<sup>2</sup> Tananaev Institute of Chemistry of Kola Science Centre, Russian Academy of Sciences, 26a Fersman Street, 184209 Apatity, Russia

<sup>3</sup> Laboratory of Nature-Inspired Technologies and Environmental Safety of the Arctic, Kola Science Centre, Russian Academy of Sciences, 14 Fersman Street, 184209 Apatity, Russia; samgleb@yandex.ru

\* Correspondence: g.ivanyuk@ksc.ru; Tel.: +7-81555-79531

Received: 30 April 2019; Accepted: 20 May 2019; Published: 22 May 2019



**Abstract:** The modal composition of (apatite)-nepheline-titanite ore and its geological setting within apatite deposits of the Khibiny Massif allow selective mining of titanite ore and its hydrochloric acidic processing. The reaction of titanite with concentrated hydrochloric acid produces hydrated titanosilicate precipitate (TSP) which, in turn, can be a precursor in titanosilicate synthesis. It is particularly noteworthy that a synthetic analogue of korobitsynite,  $\text{Na}_5(\text{Ti}_3\text{Nb})[\text{Si}_4\text{O}_{12}]_2\text{O}_2(\text{OH})_2 \cdot 7\text{H}_2\text{O}$ , was synthesized by means of TSP alteration by alkaline hydrothermal solution at 200 °C within three days. The titanosilicate obtained this way has comparatively weak cation-exchange properties regarding  $\text{Cs}^+$  and  $\text{Sr}^{2+}$  cations and considerable photocatalytic activity occurring under visible light, which allows the use of a synthetic korobitsynite analogue (SKR) for production of self-cleaning, sterilizing, and anti-fouling building materials.

**Keywords:** apatite-nepheline titanite ore; hydrochloric acidic processing; hydrated titanosilicate precipitate; hydrothermal synthesis; korobitsynite; photocatalysis

## 1. Introduction

Synthetic analogues of natural microporous titanosilicates, ETS-4 (zorite), IE-911 (sitinakite), SIV (ivanyukite), AM-4 (lintisite), etc., have many industrial applications, in particular, in waste cleaning [1,2], radionuclide conservation [3], (photo)catalysis [4,5], rare metal extraction [6,7], gas separation [8,9], and biociding [10]. Comparatively novel uses include the production of self-cleaning, sterilizing, and anti-fouling building materials (Figure 1), based on well photocatalytic activity of titanosilicates under visible light [11–17].

Our experiments with concrete tiles covered by nano-sized titanosilicate particles of ETS-4, ETS-10, IE-911, SIV, a synthetic natisite analogue and their mixtures have shown that these tiles effectively destroy organic dyes [18]. However, most of these titanosilicates are too expensive for the building industry, even when produced from local titanite concentrate using the cheapest sulfuric-acidic schema [19]. Therefore, the development of a new technology of titanite processing to obtain new titanosilicate photo-catalyzers is imperative.

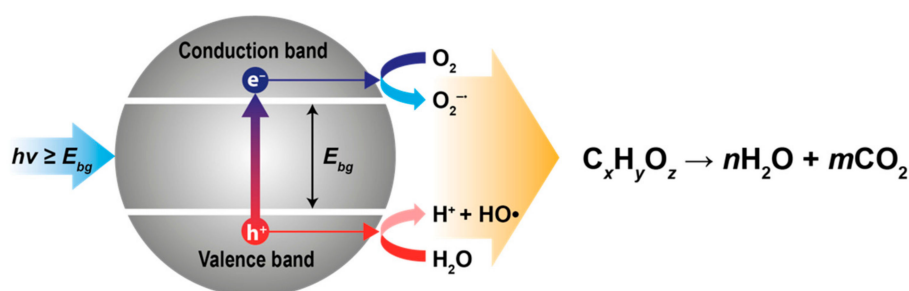


**Figure 1.** Schema of photocatalytic decomposition of organic pollutants,  $C_xH_yO_z$ , where  $h\nu$  is the light energy,  $E_{bg}$ —the band gap energy;  $h^+$  is positive hole;  $e^-$ —electron,  $O_2^{\bullet-}$ —superoxide radical;  $HO\bullet$ —hydroxyl radical.

There are a few ways to obtain cheap titanosilicate materials: (1) to use rich titanite ore without its enrichment by flotation [19]; (2) to obtain other titanosilicates with similar photocatalytic activity but lesser temperature and time of crystallization; (3) to develop another technology that would allow a complete use of titanite. All these ways were put to use in the proposed technology of hydrochloric acidic processing of titanite to produce a synthetic analogue of korobitsynite, SKR, a rhombohedral Ti-dominant member of the labuntsovite group [20].

Korobitsynite,  $Na_5(Ti_3Nb)[Si_4O_{12}]_2O_2(OH)_2 \cdot 7H_2O$ , *Pbam*,  $a$  7.349,  $b$  14.164,  $c$  7.130,  $Z = 1$  [21], was discovered by Pekov et al. [22] in a large albitized aegirine-microcline pegmatite in sodalite-nepheline syenite of Mt. Alluaiv (Lovozero Massif, Kola Peninsula). The mineral forms druses and radiated aggregates of pale-yellow semi-transparent long prismatic crystals (up to 1 cm long) grown on quartz, albite, and aegirine (Figure 2a) in voids of the pegmatite axial zone.

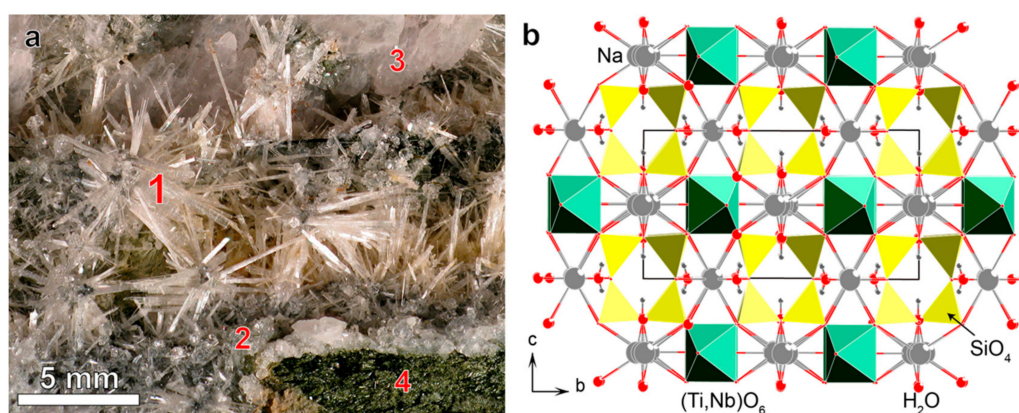


**Figure 2.** Radiated aggregates and long prismatic crystals (a) and crystal structure of korobitsynite ((b), after [21]). 1—korobitsynite, 2—quartz, 3—albite, 4—aegirine.

The crystal structure of korobitsynite (Figure 2b) is based on a titanosilicate framework consisting of chains of corner-connected  $(Ti,Nb)O_6$  octahedra (along  $a$ ) coupled by 4-member rings of  $SiO_4$  tetrahedra [21]. By analogy with other titanosilicates [11,12,15], presence of semiconductive one-dimensional ...  $Ti-O-Ti-O-Ti$  ... chains (titania quantum wires) in the framework causes the photocatalytic activity of korobitsynite. In this framework, there are four channel sets occupied by extra-framework Na cations and water molecules. A widest (FCD = 3Å) eight-membered channel (1), formed by four  $SiO_4$  tetrahedra and four  $(Ti,Nb)O_6$  octahedra, lies along  $c$ . Smaller six-membered channels (2) and (3), delimited by four tetrahedra and two octahedra, develop along  $b$ . A third six-membered channel (4), also formed by four tetrahedra and two octahedra, runs along  $a$  and intersects channel (2). The largest channel (1) is intersected by channel (3), while channel (2) intersects channel (4). In normal conditions, korobitsynite is a weak cation-exchanger because it absorbs only a

limited amount of one-two-valent metals, without crowding out initial extra-framework cations and water molecules [23].

In [24], there is presented a synthesis schema for a korobitsynite-like orthorhombic titanosilicate TR01,  $\text{Na}_{5.36}\text{Ti}_4(\text{Si}_4\text{O}_{12})_2(\text{O}_{0.34}\text{OH}_{0.66})_4 \cdot 10.31\text{H}_2\text{O}$ , *Cmmm*, *a* 7.278, *b* 14.134, *c* 7.118 Å, *Z* = 1. Hydrothermal synthesis of TR01 was performed at 230 °C during 8 days from a mixture obtained by sol-gel method: 1SiO<sub>2</sub>:0.108TiO<sub>2</sub>:0.77Na<sub>2</sub>O:0.125K<sub>2</sub>O:0.090Ce<sub>2</sub>O<sub>3</sub>:0.040SrO:0.008CaO:0.005BaO:45H<sub>2</sub>O.

In our work, we have developed an original variant of hydrothermal SKR synthesis based on composition consisting of hydrated oxides of Ti and Si, without the technically difficult sol-gel method used when obtaining the Ti-precursor. The hydrated oxides were obtained by means of hydrochloric acidic processing of titanite, which allowed, among other things, to use silica contained in this mineral (in contrast with sulfuric-acidic schema losing the silica).

## 2. Materials and Methods

### 2.1. Materials

In this study, we used blocks of rich apatite-nepheline-titanite ore of the Koashva deposit [19]. The rock consists of titanite (10–50 modal %), nepheline (15–50 modal %), fluorapatite (5–20 modal %), aegirine-augite and potassic magnesio-arfvedsonite (5–30 modal %), orthoclase and titanomagnetite (up to 5 modal %). Grain size of titanite widely ranges from 0.01 to 30 mm. The average chemical composition of titanite is (wt%): TiO<sub>2</sub> 39 ± 3, SiO<sub>2</sub> 30.1 ± 0.7, CaO 27 ± 2, FeO 1.1 ± 0.4, Nb<sub>2</sub>O<sub>5</sub> 1 ± 1, Na<sub>2</sub>O 0.7 ± 0.6, SrO 0.4 ± 0.2, Ce<sub>2</sub>O<sub>3</sub> 0.4 ± 0.2, Al<sub>2</sub>O<sub>3</sub> 0.3 ± 0.2, La<sub>2</sub>O<sub>3</sub> 0.1 ± 0.1.

The reagents used included reagent-grade hydrochloric acids, sodium and potassium hydroxides (HCl 37.5%, NaOH 99%, KOH 99%), analytical reagent grade pentahydrate sodium metasilicate, Na<sub>2</sub>SiO<sub>3</sub>·5H<sub>2</sub>O, cesium and strontium chlorides, CsCl and SrCl<sub>2</sub> (Reachem, Moscow, Russia), and distilled water (Tananaev Institute of Chemistry, Apatity, Russia). The ore blocks were crushed on a jaw crusher and milled in a 1.5 kW AGO-2 planetary mill (NOVIC, Novosibirsk, Russia) up to the powder fraction lesser than 40 μm. The chemical composition of the milled sample was determined using a FT IR 200 spectrophotometer (Perkin Elmer, Waltham, MA, USA).

### 2.2. Methods

In accordance with [19], the produced powder sample was cleaned by means of dissolution of apatite, nepheline and titanomagnetite in diluted hydrochloric acid (50 g/L) at the temperature of 50 ± 5 °C, with the solid: liquid ratio S:L = 1:4, using a magnetic stirrer for 2 h (Figure 3):



After a full dissolution of apatite and nepheline, a purified titanite-orthoclase-clinopyroxene concentrate was separated by filtration, and mixed with a concentrated hydrochloric acid (400 g/L) heated to 80 °C, with solid-liquid (weight-volume) ratio S:L = 1:3. This mixture was boiled for 10–12 h to dissolve the titanite. That step was followed by the liquid phase, separated by filtration, and, finally, titanosilicate precipitate (TSP) was produced.

The contents of Ca and Ti in the liquid phase were determined using inductively coupled plasma mass spectrometry (ICP-MS) on an ELAN 9000 DRC-e (Perkin Elmer, Waltham, MA, USA). The chemical composition of TSP was determined using a FT IR 200 spectrophotometer. The powder-like TSP was separated, washed, dried and analyzed by DSC/TGA and powder XRD methods using a STA 449 F3 instrument (NETZSCH-Gerätebau GmbH, Selb, Germany) and a XRD-6000 diffractometer (Shimadzu, Kyoto, Japan), with a Cu X-ray tube operated at 60 kV and 55 mA.

To synthesize SKR, to the water solution of  $\text{Na}_2\text{SiO}_3$  with  $\text{SiO}_2$  concentration of 125 g/L, there were added first a carefully calculated amount of NaOH (in some experiments, also KOH), and then a portion of air-dry TSP (Table 1). The suspension thus obtained was mixed for 2 h at 20–50 °C, placed in a 70-mL laboratory autoclave and held at  $200 \pm 5$  °C for 3 days. The volume of the initial mixture remained 60 mL. The produced fine-crystalline SKR was separated and, after washing, placed in a drying cabinet at  $70 \pm 5$  °C for 7–10 h.

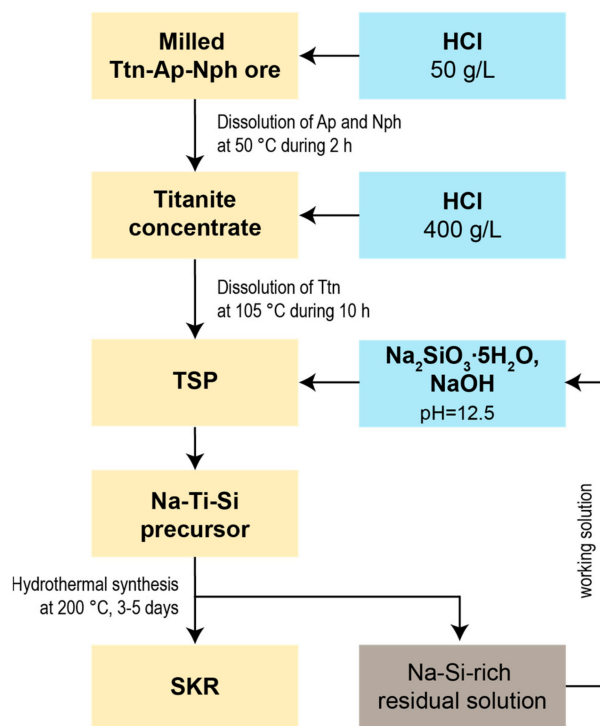


**Figure 3.** A principal scheme of apatite-nepheline-titanite ore processing for SKR synthesis.

**Table 1.** Experimental conditions of SKR synthesis.

No	$T$ , °C	$\text{TiO}_2\text{:SiO}_2$	$\text{TiO}_2\text{:Na}_2\text{O}$	$\text{TiO}_2\text{:KOH}$	pH
1	20	1:5	1:4.5	–	12.03
2	50	1:5	1:4.5	–	12.04
3	20	1:5	1:4.5	1:1	12.71
4	50	1:5	1:4.5	1:1	12.69

The modal composition of the synthesized samples was determined by means of a Shimadzu XRD-6000 diffractometer (see above). The morphology and chemical composition of SKR particles were analyzed with a scanning electron microscope Leo-1450 (Carl Zeiss Microscopy, Oberkochen, Germany) equipped with a Quantax EDS analyzer.

The surface properties and the porosity of the final products were determined by nitrogen and adsorption/desorption method at 77 K using a surface area analyzer TriStar 3020 (Micromeritics Instrument Corp., Norcross, GA, USA). Prior to adsorption/desorption measurements the samples were degassed at 120 °C for about 24 h. The pore size distributions were determined by BJH method using the desorption branch of corresponding isotherms. The pore diameter  $D_{\text{BJH}}$  was calculated as  $4 V/S$ .

To estimate the sorption abilities of the obtained products, the samples were placed for 20 h in water solutions of CsCl (1 g/L) or SrCl<sub>2</sub> (1.43 g/L), with S:L = 1:200 and a magnetic stirrer. After that, the used-up sorbent was separated and the residual contents of Sr or Cs in liquid were determined

using the ICP-MS method. The maximal sorption capacity ( $SC$ ) was estimated as:  $SC = (C_0 - C) \cdot V/m$ , where  $C_0$  with  $C$  being the initial and final contents of Cs or Sr in solution,  $V$  the volume of solution and  $m$  the weight of sorbent.

The photochemical activity of synthesized titanosilicates was determined in their suspensions with water solution of ferroin,  $[\text{Fe}^{2+}(\text{C}_{12}\text{H}_8\text{N}_2)_3]\text{SO}_4$ , illuminated by visible light and 400 nm UV-light [25,26]. In these experiments, suspension of 0.2 g of titanosilicate and 15 mL of red-colored ferroin (190 mg/L) was exposed to daylight or UV light for 3 h, then the precipitate was separated by a centrifuge (8000 rotations per minute for 5 min), and residual concentration of ferroin in the solution was determined by photocolormeter KFK 3-01 (Analitlab, Moscow, Russia) at  $\lambda = 510$  nm. Photochemical activity  $E$  was estimated as  $E = [(C_0 - C)/C_0] \times 100\%$ , where  $C_0$  and  $C$  are the initial and final ferroin content in the solution.

### 3. Results

#### 3.1. TSP Production

Hydrochloric acidic cleaning of (apatite)-nepheline-titanite ore is satisfactorily effective because both fluorapatite and nepheline are easily dissolvable in diluted HCl. The titanite concentrate obtained this way contains (wt%)  $\text{TiO}_2$  31.5,  $\text{Al}_2\text{O}_3$  1.62,  $\text{P}_2\text{O}_5$  0.21 [19]. Titanite is also well soluble in concentrated hydrochloric acid.

The highest content of Ti (and Si) in the solution is reached after 5 h, and then it begins to decrease rapidly due to the formation of TSP, while Ca remains in the liquid (Figure 4). Titanite gradually dissolves in hydrochloric acid, and a titanosilicate precipitate begins to form in the liquid phase after 5 h. A complete dissolution of titanite and TSP formation occurs after 10 h. The precipitate can be easily separated by filtration. Calcium remains in the filtrate and can be recovered as  $\text{CaCl}_2$ .

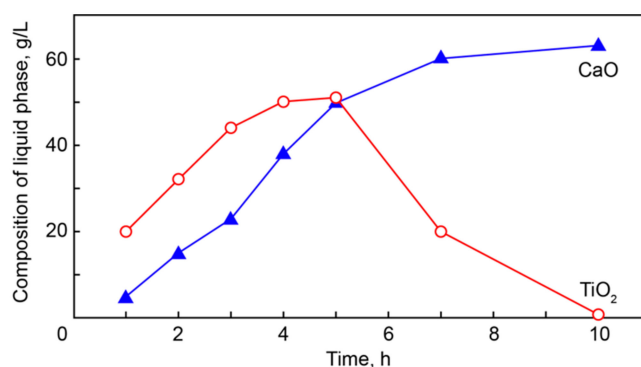


**Figure 4.** Change in Ti and Ca contents in concentrated hydrochloric acidic solution with time.

According to powder XRD and DTG data (Figure 5), dried TSP consists of nano-sized rutile and amorphous  $\text{SiO}_2 \cdot n\text{H}_2\text{O}$ , with total water content about 10 wt%. Composition of TSP after annealing at 850 °C is following (wt%):  $\text{TiO}_2$  54.19,  $\text{SiO}_2$  44.11,  $\text{Al}_2\text{O}_3$  0.47,  $\text{P}_2\text{O}_5$  0.23,  $\text{Fe}_2\text{O}_3$  0.16,  $\text{Nb}_2\text{O}_5$  0.35,  $\text{CaO}$  0.08, which determines the initial formula of TSP as  $\text{TiO}_2 \cdot \text{SiO}_2 \cdot 2\text{H}_2\text{O}$ .

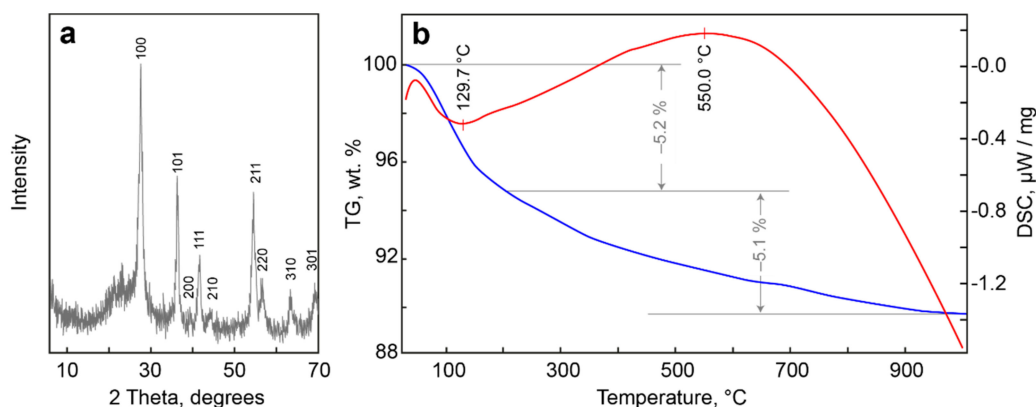


**Figure 5.** Powder X-Ray diffraction profile (a) and TG/DSC curves of TSP (b). Indexed peaks correspond to rutile.

### 3.2. SKR Synthesis

For the synthesis of SKR by means of TSP hydrothermal alteration, Na-K-rich solutions, as well as those that were Na-rich, were used (Table 2). The resulting products contain well-formed long prismatic SKR crystals accompanied by isometric globules of an amorphous titanosilicate (ATS), content of which in products 3 and 4 exceeds the SKR amount (Figure 6a). The estimation of the chemical composition of these phases (Table 3) has shown that one is close to another, but they both differ from the ideal korobitsynite by much lesser Nb amount. Also, ATS is richer in K and Ti at the expense of Na and Si, respectively.

**Table 2.** Results of SKR synthesis.

No	Filtrate				Titanosilicate Product
	pH	Volume, mL	SiO <sub>2</sub> , g/L	Na(K), g/L	
1	12.57	53	56.09	46.0 (0)	SKR >> ATS
2	12.52	56	51.68	46.4 (0)	SKR > ATS
3	12.75	53	44.54	42.8 (11.5)	ATS > SKR
4	12.75	53	55.96	46.0 (12.0)	ATS >> SKR

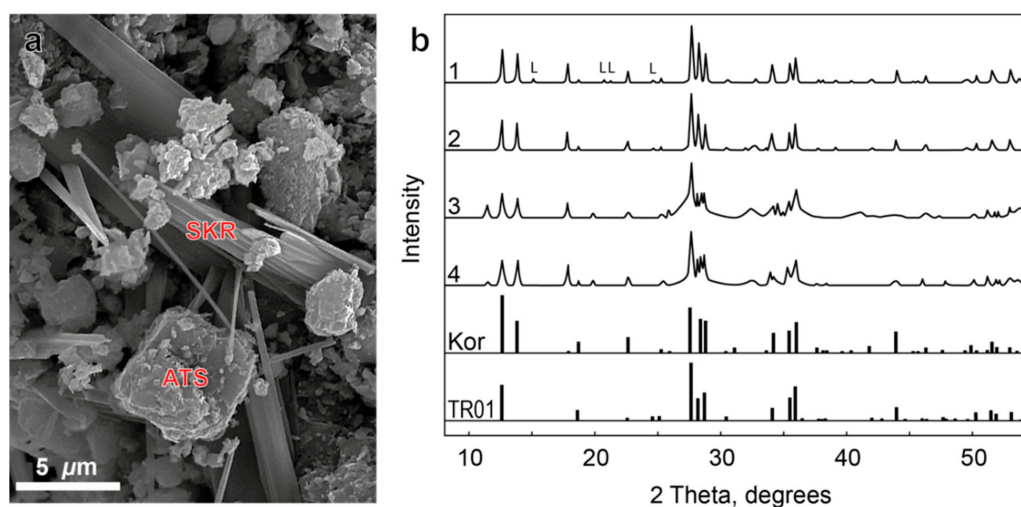


**Figure 6.** SE image of sample 3 (a) and powder X-Ray diffraction patterns of samples 1–4 in comparison with the patterns of natural korobitsynite and TR01 after [24] (b). L—lorenzenite.

**Table 3.** Chemical composition of co-existing SKR and ATS.

Constituent	H <sub>2</sub> O	Na <sub>2</sub> O	K <sub>2</sub> O	Al <sub>2</sub> O <sub>3</sub>	SiO <sub>2</sub>	Cl	TiO <sub>2</sub>	Nb <sub>2</sub> O <sub>5</sub>
SKR		15.52	–	0.67	42.22	-	41.10	0.44
ATS		12.77	2.5	0.63	34.41	0.13	49.16	0.42
Na <sub>5</sub> (Ti <sub>3</sub> Nb)[Si <sub>4</sub> O <sub>12</sub> ] <sub>2</sub> O <sub>2</sub> (OH) <sub>2</sub> ·7H <sub>2</sub> O	12.51	13.45			41.71		20.80	11.53

Figure 6b presents results of powder XRD analysis of obtained titanosilicate products in comparison with calculated XRD patterns of korobitsynite and TR01 [24]. As may be seen, all obtained titanosilicates are closely related with the natural korobitsynite, with much higher crystallinity (estimated from the sharpness of the diffraction peaks) of samples 1 and 2 (without KOH in precursor) than 3 and 4 (with KOH in the initial mixture). Samples 3 and 4 contain much more ATS, which increases the XRD background level. In potassium-free samples 1 and 2, there is an insignificant impurity of lorenzenite.

The size of SKR crystals reaches  $20 \times 3 \times 1 \mu\text{m}$ . A low specific surface area (7–19 m<sup>2</sup>/g) and general pore volume (0.03–0.08 cm<sup>3</sup>/g) of all obtained products, as well as above mentioned features of cation-exchange reactions with the SKR participant, define comparatively weak sorption properties of these mixtures. Nevertheless, the average diameter of mesopores allows to carry cation-exchange reactions with middle-sized cations. The sorption capacity of obtained products regarding Cs<sup>+</sup> and Sr<sup>2+</sup> cations (Table 4) confirmed our assumption: large Cs<sup>+</sup> cations were not sorbed in contrast with medium-sized Sr<sup>2+</sup> cations. Some higher SC values for sample 4 are probably due to surface sorption, in accordance with a greater surface area of ATS than that of SKR.

**Table 4.** Surface, sorption and photochemical characteristics of titanosilicate products.

No	S, m <sup>2</sup> /g	V, cm <sup>3</sup> /g	D <sub>BJH</sub> , nm	SC, mg/g		E, %	
				Sr <sup>2+</sup>	Cs <sup>+</sup>	Visible Light	UV Light
1	6.5 ± 0.1	0.0272 ± 0.0005	18.1 ± 0.1	56	4	31.48	44.62
2	8.9 ± 0.1	0.0372 ± 0.0001	17.7 ± 0.1	54	4	16.01	36.79
3	14.5 ± 0.1	0.0632	18.1 ± 0.1	68	18	24.24	46.5
4	18.7 ± 0.1	0.0795 ± 0.0002	17.7 ± 0.1	94	30	17.22	39.49

The comparison of an estimated photochemical activity of synthesized titanosilicate products (Table 4) with the activity of other titanosilicates (Table 5) has shown that photocatalytic activity *E* of SKR-bearing samples on visible light is compatible with that of IE-911 and SIV, and sufficiently exceeds activity of ETS-4 and, especially, of titanium oxides. This confirms the possibility to use the obtained products for production of self-cleaning building materials.

**Table 5.** Photochemical activity of mineral-like titanosilicates and titanates under visible light.

	Mixture of IE-911, ETS-4 and SIV	SIV	SKR	ETS-4	Rutile	Degussa P25
Weight, g	0.2	0.2	0.2	0.2	0.2	0.2
<i>E</i> , %	68.72	42.63	31.48	18.95	5.79	4.74

#### 4. Discussion

In our previous work, we presented a new technology of sulfuric-acidic processing of rich titanite ore (or titanite concentrate obtained by a traditional way). This technology is very effective because it utilizes sulfuric acid of nearest metallurgical combinates and produces functional titanyl sulfates as intermediate products [19]. On the other hand, sulfuric-acidic processing of titanite is accompanied by the production of large amounts of noxious waste, which can be utilized, of course, but with the obvious appreciation of the final products.

Although the proposed herein hydrochloric acidic schema is not universal, it allows one to obtain some viable products, in particular, SKR, with minimal waste. Besides, the easily obtained hydrated titanosilicate precipitate, TSP, is a handy precursor that does not require difficult sol-gel manipulations. It is also important that Na-Si-rich residual solution can be recycled.

With the photodegradation experiment having shown sound photocatalytic properties of korobitsynite, we can use this titanosilicate for environmental remediation. The first experiments have shown that incorporation of SKR photoactive nanoparticles into a cement composition results in the creation of self-cleaning surfaces and also increases the concrete's strength properties and its resistance to wear. The further steps in this direction will include reinforcing the SKR photocatalytic activity by means of Na substitution onto Au, Ag, Pt, Co, Mn and other noble and transition metals [12–14]. It must be noted also that Sr-substituted ETS-4 showed ca.4 times better photocatalytic hydrogen production than ETS-4 itself [27], thus we can expect analogue effect in Sr-substituted SKR.

## 5. Conclusions

- (1) Almost all apatite deposits of the Khibiny massifs contain sufficient reserves of (apatite)-nepheline-titanite ore, which forms lens-like bodies up to 50 m thick and above 5 km long. This is a good titanium source that can be tapped without the traditional flotation schema, but by using only acidic cleaning from soluble impurities of apatite and nepheline and insoluble clinopyroxenes ( $\pm$ microcline and amphiboles);
- (2) A new technology of hydrochloric acidic processing of titanite is now developed. It allows extraction about 90 wt% of Ti and Si into hydrated titanosilicate precipitate, TSP, while Ca and Sr remain in the chloride solution;
- (3) Hydrated TSP is a novel handy precursor for SKR synthesis by means of reaction with alkaline Na-rich hydrothermal solution at  $200 \pm 5$  °C for 3 days;
- (4) The obtained crystalline products differ from currently known synthetic compounds TR01 [24] by Nb presence and corresponding structural features, being close to natural korobitsynite;
- (5) The possibilities of SKR use include selective sorption of Sr (in contrast with IE-911, ETS-4, and SIV that favored Cs) and, mainly, photocatalytic applications, in particular, production of self-cleaning, sterilizing and anti-fouling building materials and coverings.

**Author Contributions:** L.G.G., A.I.N. and M.V.M. designed the experiments, performed ore processing and titanosilicate synthesis, and wrote the manuscript. E.S.S., G.O.K. and G.O.S. participated in the experiments. Y.A.P. performed electron-microscope investigations. G.Y.I. wrote and reviewed the manuscript. All authors discussed the manuscript.

**Funding:** The research is supported by the Kola Science Center of Russian Academy of Sciences (0226-2019-0009, 0226-2019-0011) and the Russian Foundation for Basic Research (18-29-12039).

**Acknowledgments:** We are grateful to JSC “Apatite” who helped us with titanite ore sampling. We would like to thank T.L. Panikorovskii, E.A. Selivanova and the anonymous reviewers for their suggestions and comments.

**Conflicts of Interest:** The authors declare no conflict of interest. The founding sponsors had no role in the design of the study; in the collection, analyses, or interpretation of data; in the writing of the manuscript, and in the decision to publish the results.

## References

1. Mann, N.R.; Todd, T.A. Removal of Cesium from Acidic Radioactive Tank Waste by Using Ionsiv IE-911. *Sep. Sci. Technol.* **2005**, *39*, 2351–2371. [[CrossRef](#)]
2. Milyutin, V.V.V.; Nekrasova, N.A.A.; Yanicheva, N.Y.Y.; Kalashnikova, G.O.O.; Ganicheva, Y.Y.Y.Y. Sorption of cesium and strontium radionuclides onto crystalline alkali metal titanosilicates. *Radiochemistry* **2017**, *59*, 65–69. [[CrossRef](#)]



3. Britvin, S.N.; Gerasimova, L.G.; Ivanyuk, G.Y.; Kalashnikova, G.O.; Krzhizhanovskaya, M.G.; Krivovivhev, S.V.; Mararitsa, V.F.; Nikolaev, A.I.; Oginova, O.A.; Panteleev, V.N.; et al. Application of titanium-containing sorbents for treating liquid radioactive waste with the subsequent conservation of radionuclides in Synroc-type Titanate ceramics. *Theor. Found. Chem. Eng.* **2016**, *50*, 598–606. [[CrossRef](#)]
4. Sudheesh, N.; Shukla, R.S. Rhodium exchanged ETS-10 and ETS-4: Efficient heterogeneous catalyst for hydroaminomethylation. *Appl. Catal. A Gen.* **2014**, *473*, 116–124. [[CrossRef](#)]
5. Busca, G. *Heterogeneous Catalytic Materials: Solid State Chemistry, Surface Chemistry and Catalytic Behaviour*; Elsevier: Amsterdam, The Netherlands; Oxford, UK, 2014; ISBN 978-0-444-59524-9.
6. Lopes, C.B.; Otero, M.; Coimbra, J.; Pereira, E.; Rocha, J.; Lin, Z.; Duarte, A. Removal of low concentration  $\text{Hg}^{2+}$  from natural waters by microporous and layered titanosilicates. *Microporous Mesoporous Mater.* **2007**, *103*, 325–332. [[CrossRef](#)]
7. Yanicveha, N.Y.; Ganicheva, Y.Y.; Kasikov, A.G.; Yakovenchuk, V.N.; Nikolaev, A.I.; Kalashnikova, G.O.; Ivanyuk, G.Y. The Method of Modified Pharmacosiderite-Type Titanosilicate Obtaining. Russian Patent RU-2625118, 11 July 2017.
8. Kuznicki, S.M.; Bell, V.A.; Nair, S.; Hillhouse, H.W.; Jacubinas, R.M.; Braunbarth, C.M.; Toby, B.H.; Tsapatsis, M. A titanosilicate molecular sieve with adjustable pores for size-selective adsorption of molecules. *Nature* **2001**, *412*, 720–724. [[CrossRef](#)] [[PubMed](#)]
9. Perez-Carvajal, J.; Aranda, P.; Ruiz-Hitzky, E. Titanosilicate-sepiolite hybrid nanoarchitectures for hydrogen technologies applications. *J. Solid State Chem.* **2019**, *270*, 287–294. [[CrossRef](#)]
10. Pérez-Carvajal, J.; Lalueza, P.; Casado, C.; Téllez, C.; Coronas, J. Layered titanosilicates JDF-L1 and AM-4 for biocide applications. *Appl. Clay Sci.* **2012**, *56*, 30–35. [[CrossRef](#)]
11. Llabrés i Xamena, F.X.; Calza, P.; Lamberti, C.; Prestipino, C.; Damin, A.; Bordiga, S.; Pelizzetti, E.; Zecchina, A. Enhancement of the ETS-10 titanosilicate activity in the shape-selective photocatalytic degradation of large aromatic molecules by controlled defect production. *J. Am. Chem. Soc.* **2003**, *125*, 2264–2271. [[CrossRef](#)]
12. Guan, G.; Kida, T.; Kusakabe, K.; Kimura, K.; Abe, E.; Yoshida, A. Photocatalytic reactivity of noble metal-loaded ETS-4 zeolites. *Inorg. Chem. Commun.* **2004**, *7*, 618–620. [[CrossRef](#)]
13. Uma, S.; Rodrigues, S.; Martyanov, I.N.; Klabunde, K.J. Exploration of photocatalytic activities of titanosilicate ETS-10 and transition metal incorporated ETS-10. *Microporous Mesoporous Mater.* **2004**, *67*, 181–187. [[CrossRef](#)]
14. Krisnandi, Y.K.; Howe, R.F. Effects of ion-exchange on the photoreactivity of ETS-10. *Appl. Catal. A Gen.* **2006**, *307*, 62–69. [[CrossRef](#)]
15. Shiraiishi, Y.; Tsukamoto, D.; Hirai, T. Selective photocatalytic transformations on microporous titanosilicate ETS-10 driven by size and polarity of molecules. *Langmuir* **2008**, *24*, 12569–12663. [[CrossRef](#)]
16. Macphee, D.E.; Folli, A. Photocatalytic concretes—The interface between photocatalysis and cement chemistry. *Cem. Concr. Res.* **2016**, *85*, 48–54. [[CrossRef](#)]
17. Tyukavkina, V.V.; Gerasimova, L.G.; Semushin, V.V. Properties of compositions based on cement and modified nanodispersed titanium dioxide. *Inorg. Mater. Appl. Res.* **2019**, *10*, 122–126. [[CrossRef](#)]
18. Tyukavkina, V.V.; Gerasimova, L.G.; Tsyryateva, A.V. Synthetic titanosilikatny additives for special cement composites. *Perspektivnye Materialy* **2019**, *4*, 40–48. [[CrossRef](#)]
19. Gerasimova, L.; Nikolaev, A.; Maslova, M.; Shchukina, E.; Samburov, G.; Yakovenchuk, V.; Ivanyuk, G. Titanite Ores of the Khibiny Apatite-Nepheline-Deposits: Selective Mining, Processing and Application for Titanosilicate Synthesis. *Minerals* **2018**, *8*, 446. [[CrossRef](#)]
20. Chukanov, N.V.; Pekov, I.V.; Zadov, A.E.; Voloshin, A.V.; Subbotin, V.V.; Soroktina, N.V.; Rastsvetaeva, R.K.; Krivovichev, S.V. *Minerals of the Labuntsovite Group*; Nauka: Moscow, Russia, 2003; ISBN 5-02-006441-6. (In Russian)
21. Rastsvetaeva, R.K.; Chukanov, N.V.; Pekov, I.V. Crystal structure of a new mineral, titanium analogue of orthorhombic nenadkevichite. *Dok. RAN* **1997**, *357*, 364–367. (In Russian)
22. Pekov, I.V.; Chukanov, N.V.; Khomyakov, A.P.; Rastsvetaeva, R.K.; Kucherinenko, Y.V.; Nedel'ko, V.V. Korobitsynite  $\text{Na}_{3-x}(\text{Ti,Nb})_2[\text{Si}_4\text{O}_{12}](\text{OH},\text{O})_2 \cdot 3-4\text{H}_2\text{O}$ —a new mineral from Lovozero Massif, Kola Peninsula. *ZVMO* **1999**, *3*, 72–79. (In Russian)
23. Zolotarev, A.A. Crystal Chemistry of the Lovozeroite and Labuntsovite Group Minerals. Ph.D. Thesis, St. Petersburg University, St. Petersburg, Russia, 2007.
24. Cadoni, M.; Ferraris, G. Microporous titanosilicates—Synthesis and structural characterization of a new orthorhombic-type labuntsovite. *Eur. J. Mineral.* **2007**, *19*, 217–222. [[CrossRef](#)]

25. Kozlova, E.A.; Kozhevnikova, N.S.; Cherepanova, S.V.; Lyubina, T.P.; Gerasimov, E.Y.; Kaichev, V.V.; Vorontsov, A.V.; Tsybulya, S.V.; Rempel, A.A.; Parmon, V.N. Photocatalytic oxidation of ethanol vapors under visible light on CdS–TiO<sub>2</sub> nanocatalyst. *J. Photochem. Photobiol. A Chem.* **2012**, *250*, 103–109. [[CrossRef](#)]
26. Sedneva, T.A.; Belikov, M.L.; Belyaevskii, A.T. Synthesis and study of photocatalytic oxide nanocomposites of titanium (IV) and cobalt (II). *Theor. Found. Chem. Eng.* **2016**, *50*, 498–507. [[CrossRef](#)]
27. Shankar, M.V.; Ye, J.H. Green-Chemical Synthesis of ETS-4 Zeotypes for Photocatalytic Hydrogen Production. *Adv. Mater. Res.* **2012**, *584*, 366–370. [[CrossRef](#)]



© 2019 by the authors. Licensee MDPI, Basel, Switzerland. This article is an open access article distributed under the terms and conditions of the Creative Commons Attribution (CC BY) license (<http://creativecommons.org/licenses/by/4.0/>).